DOI: 10.13009/EUCASS2019-259

Near-field sonic boom signature measurement system for AVIC ARI's FL-60 wind tunnel

Liu Zhongchen [1, 2], Qian Zhansen [1, 2,*], Leng Yan [1, 2]

1. AVIC Aerodynamics Research Institute, Shenyang, 110034, China

2. Aviation Key Laboratory of Science and Technology on High Speed and High Reynolds Number Aerodynamic Force Research, Shenyang, 110034, China

Abstract

Based on AVIC ARI's FL-60 wind tunnel, the measurement systems were conducted to get the sonic boom near-field pressure signatures efficiently and accurately. FL-60 is a trisonic, blowdown wind tunnel. The Mach number range is of 0.3 to 4.2, and the size of the test section is 1.2m × 1.2m. According to the characteristic of the wind tunnel, a pressure measurement rail equipment has been designed to instead of the traditional pressure probe to improve the measurement efficiency drastically. The shape, size and location of the pressure rail were optimized by the CFD simulation to get the best measured data. In order to reduce the flow field distortions, the "reference run" and "spatial averaging" techniques were utilized. The sonic boom near-field pressures for Seebass-ALR revolutionary model were obtained at Mach number of 1.5, 1.8 and 2.0. The test results showed that the experimental techniques for AVIC ARI's FL-60 wind tunnel are feasible and reliable.

1. Introduction

Currently, civil flight at supersonic speed is prohibited over land for many countries over the word. The primary reason is the sonic boom annoyance and potential structural damage caused by large pressure waves when the aircraft flights at speeds greater than the speed of sound [1]. It is generally recognized that the sonic boom is one of the most important questions concerning the future of supersonic aircraft, particularly with regard to commercial air transportation. The measurement of the off-body pressure signatures of the low-boom supersonic vehicles modern in wind tunnel is challenging [2-7]. The testing in wind tunnel often provides measurements of the off-body pressure signatures from less than one to several body lengths away from the model. So, the aircraft configuration must be accurately represented at very small scales and the near-field off-body pressure signatures must be measured accurately with minimal interference from the wind tunnel flow field. In addition, the model shock waves must have no distortion between the model and the measuring devices [8].

DOI: 10.13009/EUCASS2019-259

Historically, the conical probe was used to measure static pressure at a single point in the flow field when the off-body pressure signatures were measured in a wind tunnel [2]. This technique requires axial translation of the model past the probe or translation of the probe past the model to obtain the whole off-body pressure signatures of the model. The one disadvantage of this single point measurement method is time-consuming. For a continuous flow wind tunnel, in order to ensure the data accuracy, the pressure oversampling time has better up to 30 seconds, and the measurement points desired on a model are at least 80~100. The whole run time to the exclusion of the equipment movement is about 50~60 minutes per signature obviously. The other disadvantage of this single point measure method is prone to reduced data accuracy. The tunnel conditions which contribute to reduce data quality (humidity, turbulence, ambient pressure variations and stream angle) change over such long times.

Ideally, measurement equipment should measure an entire signature all at once. Unlike single-point conical probes, hundreds of pressure orifices which are used to measure a model's entire off-body pressure signature at one location of the model in the wind tunnel are laid on the surface of the pressure rail. Compared with conventional single conical probe, pressure rail has significant advantages in efficiency and precision.

In the present paper, based on AVIC ARI's FL-60 wind tunnel, some experimental techniques were conducted to get the sonic boom near-field pressure signatures efficiently and accurately, including introduction of FL-60 wind tunnel, the model and instrumentation, test technologies and experimental results. A non-reflection pressure measurement rail is used to improve the measurement efficiency drastically, and the size and location of the pressure rail is optimized by the CFD simulation. The axial movement mechanism enables the model to move forward and backward along the wind tunnel test section. The "reference run [9, 10]" and "spatial averaging [9, 10]" technique were used to reduce the flow field distortions. The sonic boom near-field pressures for Seebass-ALR standard model were obtained at Mach number of 1.5, 1.8 and 2.0. The test results showed that the experimental techniques used for AVIC ARI's FL-60 wind tunnel were feasible and reliable.

2. Introduction of AVIC ARI's FL-60 wind tunnel

FL-60 is a trisonic wind tunnel, as shown in Fig. 1. It is composed of butterfly valve, expansion joint, pressure regulating valve, large-angle expansion section, settling chamber, contraction section, flexible wall nozzle, transonic test section, supersonic diffusion section, ejector, subsonic diffusion section, muffler, etc. The length of the wind tunnel is about 92 meters.

Fig. 1 FL-60 Wind tunnel

DOI: 10.13009/EUCASS2019-259

The range of Mach number is 0.3 to 4.2, and the size of the test section is 1.2m × 1.2m. For supersonic condition, a 2-D flexible nozzle with deformable contour flat is utilized to realize Mach number 1.3-4.2 undiscretely. The experimental capabilities of FL-60 include conventional force test/pressure test, air intake test, unsteady flow test at high angle of attack, dynamic derivative test, large amplitude oscillation test, external store force test, component force test, hinge-moment test, half model supporting, aeroelasticity simulation, CTS, PSP, TSP, IR, schlieren and etc.

The wind tunnel design indexes are as follows:

(1) Test section size

Transonic: 1.2m × 1.2m × 3.8m (width × height × length)

Supersonic: 1.2m × 1.2m × 2.2m (width × height × length)

(2) Mach number range

Ma=0.3~4.2

(3) Mach number control accuracy

$\Delta Ma \leq \pm 0.0015$ $(0.3 \leq Ma \leq 1.2)$

$\Delta P_{0\,max}/P_0 \leq 0.3\%$ $(1.5 \leq Ma \leq 4.2)$

As shown in Fig. 2, the FL-60 wind tunnel is equipped with PSI8400 pressure measurement system, which is a highly modular measurement system. Equipped with different range of electronic pressure scanners, each scanner has 64 channels. The main technical parameters of PSI8400 pressure measurement system are as follows:

(1) Pressure scanning rate: 50000CH/S;

(2) Temperature range: -25℃~80℃;

(3) Pressure range: 1PSI、2.5PSI、5PSI、10PSI、15PSI、30PSI、75PSI、150PSI;

(4) Pressure measurement accuracy: 0.05%FS;

(5) Total number of channels: 1024CH.

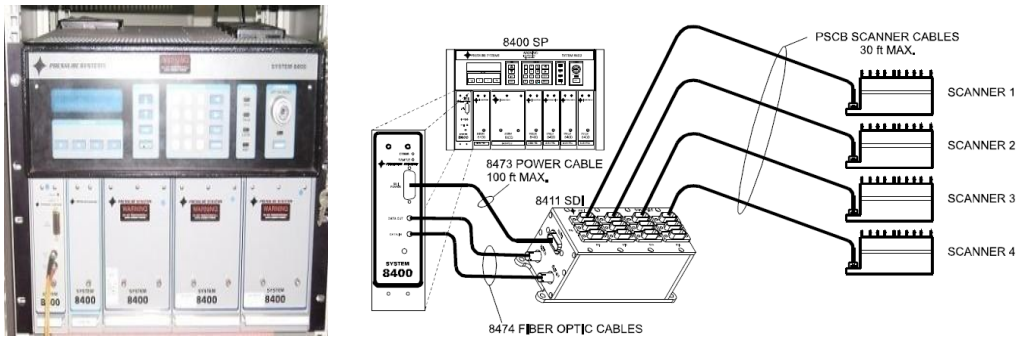

Fig. 2 PSI8400 pressure measurement system

3. Model and instrumentation

Fig. 3 gives the test design plan. The pressure rail is installed in the side wall through the removable viewing windows. The model is in the center of the wind tunnel. It can move forth and back through axial movement mechanism, and move up and down through height direction movement mechanism.

DOI: 10.13009/EUCASS2019-259

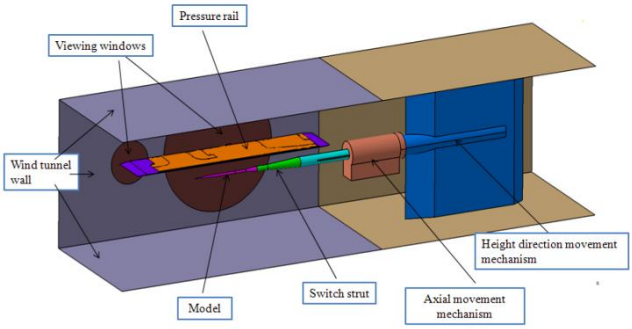

Fig.3 The test design plan

3.1 Model

A low boom low drag axisymmetric Seeb-ALR model which is designed after the work of Seebass, George and Darden [11] is used as test model. The characteristic length of this model is 224.5mm, and the diameter of this model is 17.714mm. Fig. 4 shows the geometry of the Seeb-ALR model. It is observed that the pressure signatures of this model exists small flat pressure region behind the nose shock. The flat-top pressure signatures have great advantage in revealing and understanding the measurement distortions.

Fig. 4 The geometry of the Seeb-ALR model

Seeb-ALR model is slender needle-like. It is easy to deform and difficult to manufacture. Therefore, the model is divided into two parts in the process, and then the model is connected with pins. Finally, the shape size of the model is tested by a three-dimentional measuring instrument to ensure the accuracy of the model, as shown in Fig. 5.

Fig. 5 The photograph of the Seeb-ALR model

DOI: 10.13009/EUCASS2019-259

3.2 Design of pressure rail

Pressure rail has the advantage of measuring all the off-body pressure signatures at once, since hundreds of pressure orifices are laid on the surface of it. Although this measurement technique avoids the problem which is need long period of time to take signatures, it introduces other problems. Firstly, the bow shock wave generated by the pressure rail crosses the model shock waves and distorts them, although this phenomenon depends on placement of the rail relative to the model. Secondly, due to the exist of top surface of the pressure rail, the measured data on a rail are magnified by the reflection factor. If the top surface of the pressure rail is an infinitely-thin surface, the reflection factor is 1 which means non-reflection. Similarly, if the top surface is an infinitely-wide flat plate, the reflection factor is 2 which means total reflection. Furthermore, the shock reflection of the wind tunnel wall and turbulence boundary layer effect must be considered during measuring off-body pressure signatures.

Based on the theory of static pressure conical probe, the concept of non-reflective pressure rail (RF1) will be realized [9, 10, 12]. The RF1 rail has a small rounded tip and is blade-like with a small angle from the tip to the base, and its measurement orifices facing into the flow. Because the upper edge is small (3 mm in diameter) and round, it will not has great influence on the flow field to increase measurement amplitude in measurement. The measurement upper edge is transited to 24mm width at its base gradually, and with a 3.5 degree angle from the tip to the base in order to minimize flow disturbance, the cross-section for the whole length need to keep slim. Fig.6 is the cross section of the rail. The rail has a radius tip and is 1.81m long with measured section 1.65m long. The rail height (353mm) is selected to prevent turbulence boundary layer effect and contamination of the aft part of a model's signature measured on the rail by reflections off the tunnel wall of model shock waves from the forward part of the model. The RF1 pressure rail consists of 375 pressure orifices spaced 4 mm apart, each with an internal diameter of 1.0mm. Fig.7 is the whole view of the rail.

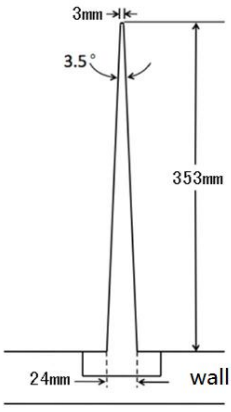

Fig. 6 Cross section of the rail

DOI: 10.13009/EUCASS2019-259

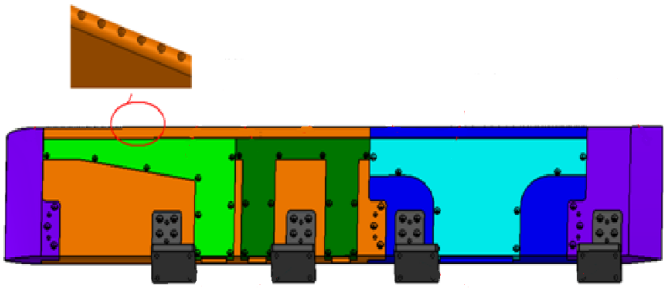

Fig. 7 The whole view of the rail

3.3 Pressure measurement instrumentation

The PSI8400 pressure measurement system was utilized to measure the off-body pressures in the wind tunnel test. As shown in Fig. 8, the measuring tubes of the scanners are connected with the orifices of the pressure rail, and the reference tubes of the scanners are connected with an orifice upstream of the pressure rail on the side wall of the test section. The reference tubes of the scanners are connected with an absolute pressure sensor through a three-way connection. During the test, the pressure signatures are measured at the same time by the scanners and the absolute pressure sensor, and the pressure distribution on the pressure rail can be obtained. The range of the scanners utilized in the test is 2.5 PSID with an accuracy of 0.05% FS, that means the measuring accuracy of the scanners is 8.62 Pa. The range of the absolute pressure sensor utilized to measure the the reference pressure of the scanners is 5 PSIA with an accuracy of 0.02%FS, that means the measuring accuracy of the absolute pressure sensor is 6.89Pa.

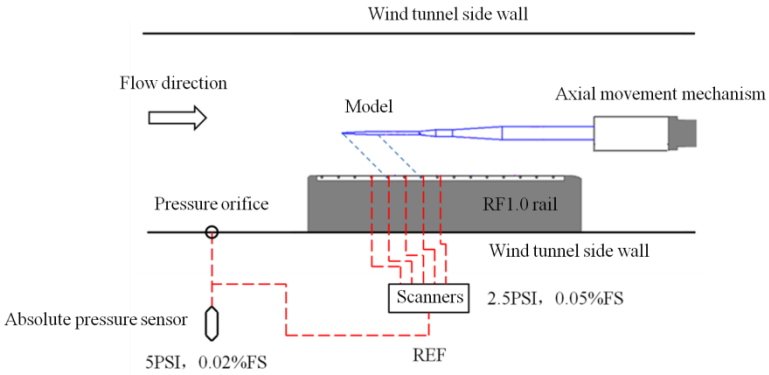

Fig. 8 The pressure measurement instrumentation

4. CFD verification

The test plan and pressure rail must be verified by CFD before manufacture. According to the wind tunnel test, the calculation conditions are given in table 1. Based on the test process, CFD verification is carried out in the following three steps. Firstly, it is to simulate the case without model as the same as the reference correction and to analyze the characteristic of flow field with only the wind tunnel wall and pressure rail in the calculation domain. Secondly, it is to simulate the case with model. The calculation results will indicate whether meeting

DOI: 10.13009/EUCASS2019-259

the test requirement. Finally, the simulation Mach number is changed to verify the result and law obtained in the second step.

Table 1 Calculation conditions

Case	Ma	Static pressure/Pa	Model
1	1.8	29978.9	√
2	1.8	29978.9	×
3	1.5	40021.4	√
4	1.5	40021.4	×

The pressure contours of pressure rail and wall for case2 and case4 is shown in Fig. 9, where the curve is the pressure signature on the upper surface of the pressure rail. It can be seen from the figure that the pressure signature on the upper surface of the pressure rail can be divided into three parts for all Mach number. A is the part affected by the compression region formed by the leading edge of the pressure rail. B is the region undisturbed by strong shock wave. C is the high pressure region formed by reflected shock wave from the wind tunnel wall. The model is located at a certain distance above the pressure rail during the test. During the wind tunnel test, it is better to let the pressure characteristic of model located in region B. Furthermore, the CFD verifies whether the design of the pressure rail and reference correction meet the test requirements.

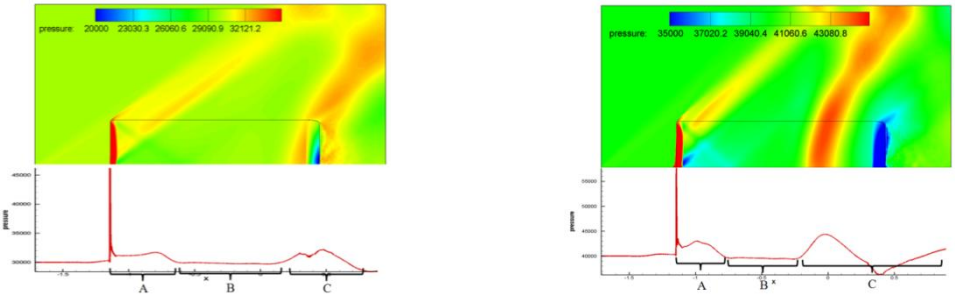

(a) Case2 (b) Case4

Fig. 9 Pressure contours of pressure rail and wall

The case1 simulation is with the model offset 0.24m downstream of the rail leading edge, and at h=0.247m. The computational result of the model, pressure rail, and tunnel wall is shown in Figure 10. The model crosses the compression region of the rail leading edge, and the pressure signature of the model is located at region B. The model's leading shock reflects from the wall far downstream of the model pressure signature on the rail. In order to obtain accurate signature, an additional computation which is the model in free-field (without the rail and wall) is run in the same position. The pressure signature along the rail is extracted from the three solutions and plotted in Figure 11(a). Subtracting the rail and wall solution from the model, rail, and wall computation yields the pressure signature of the model. The result compared with the free-field computation is shown in Figure 11(b). The computation shows that the pressure rail provides a good pressure rail design without any indication of reflection from the rail. The reference correction meets the test requirements.

DOI: 10.13009/EUCASS2019-259

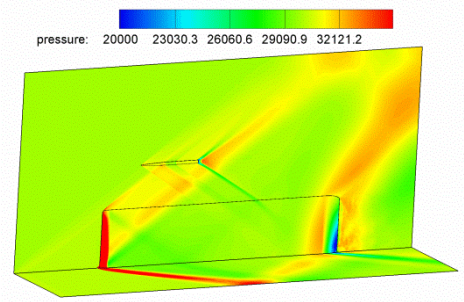

Fig. 10 Pressure contours of the case1

The above conclusion is verified by case4. The computational result of the model, pressure rail, and tunnel wall is shown in Figure 12. The pressure signature along the rail is extracted from the three solutions and plotted in Figure 13(a). Subtracting the rail and wall solution from the model, rail, and wall computation yields the pressure signature of the model. The result compared with the free-field computation is shown in Figure 13(b). The computation shows that the pressure rail provides a good pressure rail design without any indication of reflection from the rail, which further validates the conclusions obtained above.

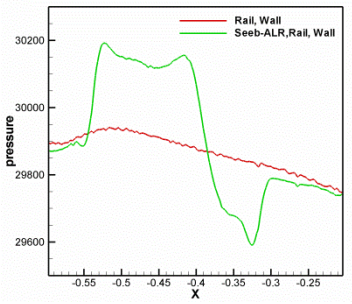

(a) Seeb-ALR, pressure rail, and tunnel wall

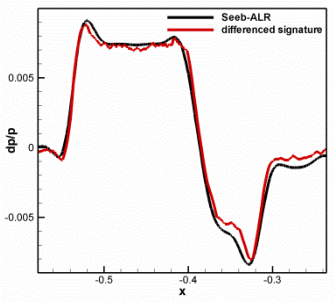

(b) Predicted signatures of pressure rail

Fig. 11 Results of Seeb-ALR, pressure rail, and tunnel wall for case1

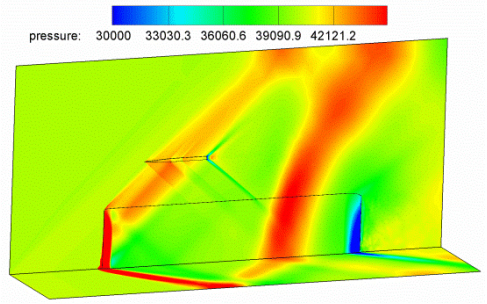

Fig. 12 Pressure contours of the case4

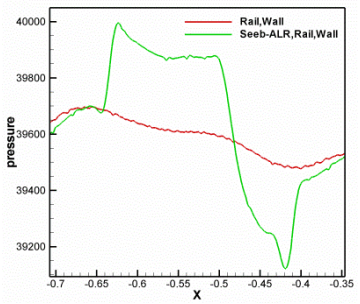

(a) Seeb-ALR, RF1 rail, and tunnel wall

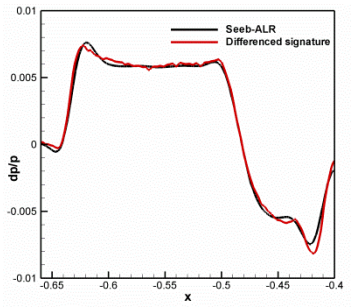

(b) Predicted signatures of RF1 rail

Fig. 13 Results of Seeb-ALR, pressure rail, and tunnel wall for case4

DOI: 10.13009/EUCASS2019-259

5. Test techniques

Compared with the traditional pressure rail, the non-reflection pressure rail is slender and has less interference to the flow field. However, for the measurement of sonic boom signatures the exist of the RF1.0 rail still leads to errors that can not be ignored. Therefore, the interference caused by the pressure rail must be corrected by reference run. The main purpose of this method is to eliminate the interference of the pressure rail on the flow field and ensure that the measurement results are only the signatures generated by the model. In addition, all supersonic wind tunnels have some weak shock wave due to factors such as wind tunnel manufacturing defects, which results in a certain non-uniformity of the flow field in the wind tunnel, and the variation of the total pressure in the front chamber leads to some unsteady characteristics of the flow field in the wind tunnel. These effects must be considered in the measurement of sonic boom signatures. Therefore, the spatial averaging technique is utilized in the test to reduce the effect of the non-uniformity of the flow field.

5.1 Reference Run

One key technique for acquiring sonic boom data using the pressure rail is that the measured data must be corrected with the reference data[9,10]. The primary purpose is to guarantee that the final data measured only the model's signatures and not the interference caused by the pressure rail or the ambient free stream signatures from the tunnel flow. The reference test introduces the concept of "clean" wind tunnel. That is, the model and support devices are either out of the wind tunnel during one test (but this is usually not necessary), or the model is moved far enough away from the rail to keep model shocks off the pressure rail or toward the rear.

Fig. 14 is the schematic diagram of the model position in the reference and measuring data test. When the model is in the reference test position, the shocks are behind the pressure rail. Accordingly, when the model is in the measuring position, the shocks fall on the instrumented section of the pressure rail. It is clear that the distance is far enough between measuring data and reference data. It is well known that the disturbance in the supersonic flow field cannot propagate forward, so it will not pollute the measured data.

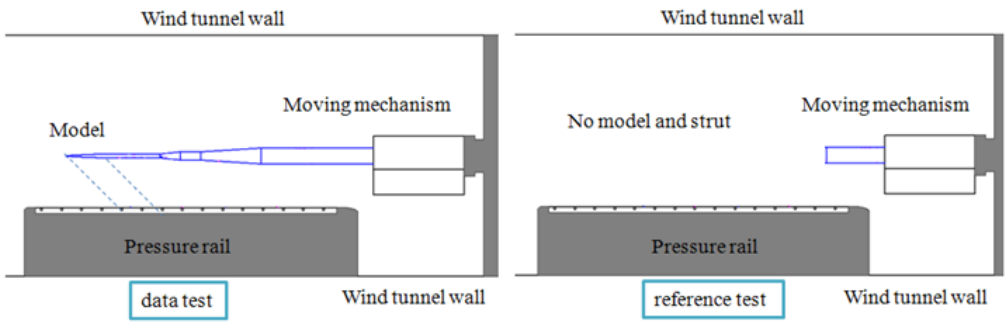

Fig. 14 Layout of reference and data test in FL-60 wind tunnel

The standard definition of $\frac{dP}{P} = \frac{P_{rail} - P_{\infty}}{P_{\infty}}$ is utilized for the sonic boom tests, P_{rail} is pressures measured on the rail, P_{∞} is the tunnel free-stream static pressure. When the model is in the measuring position, the measuring

DOI: 10.13009/EUCASS2019-259

data $(\frac{P_{rail}-P_\infty}{P_\infty})_{data}$ is obtained, and when the model is in the reference position, the reference data $(\frac{P_{rail}-P_\infty}{P_\infty})_{ref}$ is obtained. The near-field sonic boom overpressure (denoted by f_i) is obtained from

$$f_i = (\frac{P_{rail}-P_\infty}{P_\infty})_{corrected} = (\frac{P_{rail}-P_\infty}{P_\infty})_{data} - (\frac{P_{rail}-P_\infty}{P_\infty})_{ref} \quad (1)$$

5.2 Spatial averaging

All supersonic wind tunnels have non-uniformity characteristics. Figure 15 shows the schlieren image of AVIC ARI's FL-60 wind tunnel. From the figure, we can see that there are some weak shock waves in the flow field. Affected by these weak shock waves, the flow field parameters such as Mach number, flow angle and pressure are not absolutely uniform in space, and with the variation of total pressure in the wind tunnel, these flow field parameters also show some unsteady characteristics in time. In order to reduce the effect of the non-uniform disturbance of wind tunnel flow field on the measurement of sonic boom signatures, the spatial averaging technique is utilized in the tests, as shown in Figure 16.

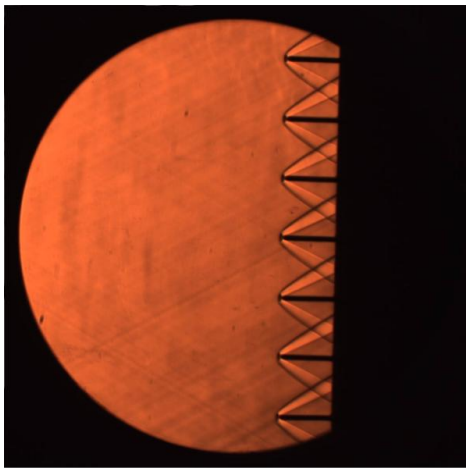

Fig. 15 The schlieren image of AVIC ARI's FL-60 wind tunnel

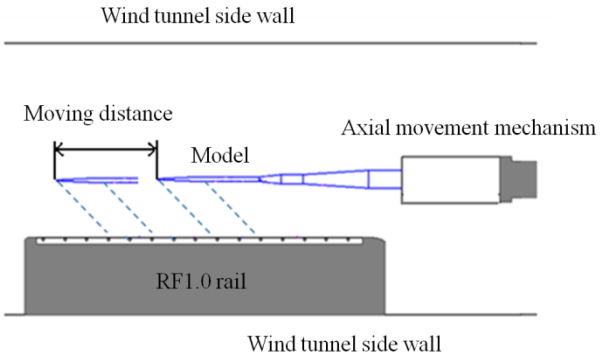

Fig. 16 The sketch of spacial averaging

The spacial averaging technique is that the model moves along the axial dimention (X-sweep) at a certain distance above the pressure rail, measures N signatures at different positions, and then aligns each series of pressure signatures so that simple averaging of the data could be accomplished. Simply stated, an averaged signature $\bar{f}$ is obtained by summing the signatures at each port f_i and dividing by the number of positions N.

$$\bar{f} = \frac{\sum f_i}{N} \quad (2)$$

DOI: 10.13009/EUCASS2019-259

The spatial averaging technique[9,10] was developed to reduce the effect of tunnel flow field spatial distortions on the data at single model positions during supersonic wind tunnel testing. It is conducted by averaging data at several positions in the fore and aft direction for an "X-sweep". The X locations at each point on the individual signatures need to be aligned in order to enable the averaging. For an X-sweep, the X values of the rail orifice locations are aligned by simply adding the moving distance ($x_{aligned} = x_{orif} + x_{mov}$).

6. Experimental results

Based on above analysis, experimental data for Seebass-ALR model obtained in the FL-60 wind tunnel is presented in this section, and the test model and instrumentation are shown in figure 17. The non-reflection pressure rail is installed on the wind tunnel side wall, and the model is connected to the axial movement mechanism which is fixed on the wind tunnel strut. The model can move forth and back above the pressure rail through automatic control. The model is at an altitude of 1.14 body length from the rail at h=247mm. The test Mach number is 1.5, 1.8, 2.0 separately. The test conditions are given in table 2. For the reference runs of 1126, 1129 and 1130, 20 individual measurements without model are obtained at different times in each run, and the averaged result of 20 measurements as the reference data. For the data runs of 1127, 1128 and 1131, 20 individual measurements with model in different axial positions are obtained in each run. So the individual corrected signature can be obtained with subtracting the reference data from the individual measurement, and then the averaging of all individual corrected signatures could be accomplished.

(a) model (b) non-reflection pressure rail

Fig. 17 Photograph of the wind tunnel test

Table 2 Test conditions

Run number	Ma	Model
1126	1.5	×
1127	1.5	√
1128	1.8	√
1129	1.8	×
1130	2.0	×
1131	2.0	√

DOI: 10.13009/EUCASS2019-259

A reference run with the model and strut moved away from the wind tunnel is necessary during the wind tunnel test. Figure 18 shows the procedure used to obtain experimental pressure signatures with non-reflection pressure rail for Mach number of 1.5. The tunnel static pressure is used as the free-stream value in dp/p. As shown in Figure 18(a), the green line is the averaged reference data of run 1126 without model, and the red line is an individual measurement result of run 1127 with model. Figure 18(b) is the differenced signatures of the model obtained by subtracting the reference run from the data run. It is observed that the individual signature have oscillations caused by the irregular tunnel ambient flow field.

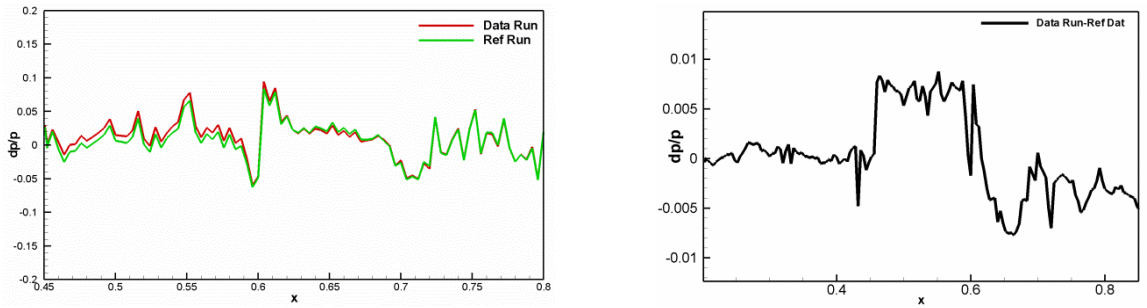

(a) pressure signatures for data and reference run (b) differenced pressure signatures

Fig. 18 The use of reference run (Ma=1.5)

In order to reduce the effect of tunnel flow field distortions on the data at fixed axial location, "spatial averaging" of x-sweep is used during test. The model is axial translated 4 orifices equating 16 mm at a time. The averaged results in a series of 20 positions compared with CFD simulation are shown in Figure 19 for all Mach numbers. From Figure 14, it is observed that "spatial averaging" can reduce distortions effectively. We can see that with the increase of Mach number, the near-field sonic boom overpressure of Seeb-ALR model increases. But the averaged signatures for all Mach numbers have small oscillations yet. By increasing the number of spacial averaging measurements, the distortion of measurement results can be further reduced and the accuracy of measurement data of sonic boom test can be improved. Furthermore, the designed pressure rail has indeed non-reflection nature and the test plan is feasible and reliable.

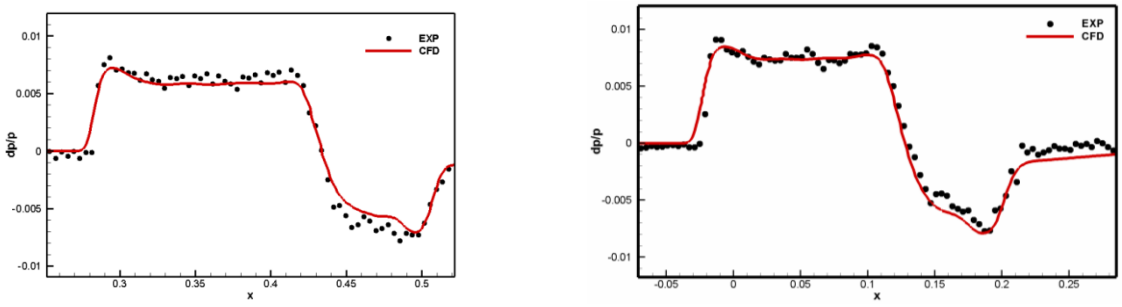

(a) Ma=1.5 (b) Ma=1.8

DOI: 10.13009/EUCASS2019-259

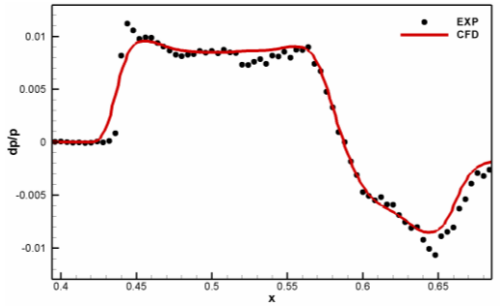

(c) Ma=2.0

Fig. 19 Averaged experimental pressure signatures compared with CFD simulation

7. Conclusions

Based on the AVIC ARI's FL-60 blow-down trisonic wind tunnel, near-field sonic boom signature measurement system is developed, including the design of non-reflection pressure measurement rail, high accuracy pressure measurement instrumentation, reference test method and spacial averaging technique. With CFD evaluation and wind tunnel test of Seeb-ALR low boom model, the successful design of the non-reflection rail is verified, and the Seeb-ALR test results show that the experimental techniques utilized for AVIC ARI's FL-60 wind tunnel are feasible and reliable.

According to the characteristics of short test time and large gas consumption of the blow-down wind tunnel, the non-reflection pressure rail is designed to instead of the traditional pressure probe, which greatly improves the measurement efficiency.

The pressure measurement instrumentation is consisted of several electronic pressure scanners which range is 2.5 PSID with an accuracy of 0.05% FS and an absolute pressure sensor which range is 5 PSIA with an accuracy of 0.02% FS. These ensure that the measurement accuracy of this system is less than 10 Pa.

To get the best measured data, the shape, size and location of the pressure rail are optimized by the CFD simulation at Mach number of 1.5 and 1.8. In order to avoid the impact of the front shock wave of the rail and the reflected shock wave from the tunnel wall, the model signature should be located in the middle of the measurement section of the pressure rail by controlling the axial movement mechanism.

The sonic boom near-field pressures for Seebass-ALR model are obtained at Mach number of 1.5, 1.8 and 2.0. To reduce the flow field distortions, the "reference run" and "spatial averaging" techniques are utilized. The test results show that the flow field interference caused by the rail can be eliminated by subtracting the reference data from the measurement data. And spacial averaging technique can significantly reduce the measurement distortion caused by the non-uniformity of wind tunnel flow field, greatly improve the accuracy of near-field pressure measurements.

DOI: 10.13009/EUCASS2019-259

References

[1] Durston D A, Elmiligui A A, Cliff S E, Winski C S, Carter M B, and Walker E L. Experimental and computational sonic boom assessment of Boeing N+2 low boom models. AIAA 2014-2140.

[2] Mack R J. An Analysis of Measured Sonic-Boom Pressure Signatures From a Langley Wind-Tunnel Model of a Supersonic-Cruise Business Jet Concept, NASA TM-2003-212447.

[3] Graham D H, Dahlin J A, Page J A, Plotkin K J, Coen P G. Wind Tunnel Validation of Shaped Sonic Boom Demonstration Aircraft Design. AIAA 2005-7.

[4] Mack R J, Method for Standardizing Sonic-Boom Model Pressure Signatures Measured at Several Wind-Tunnel Facilities. NASA TM-2007-21485.

[5] Furukawa T, Makino Y, Noguchi M, Ito T. Supporting System Study of Wind-Tunnel Models for Validation of Aft-Sonic-Boom Shaping Design. AIAA 2008-6596.

[6] Elmiligui A, Wilcox F, Cliff S, Thomas S. Numerical Predictions of Sonic Boom Signatures for a Straight Line Segmented Leading Edge Model. Seventh International Conference on Computational Fluid Dynamics (ICCFD7) Big Island, Hawaii, July 9-13, 2012, ICCFD7-2004.

[7] Wilcox F J, Elmiligui A A, Wayman T R, Waithe K A, Howe D C, Bangert L S. Experimental Sonic Boom Measurements on a Mach 1.6 Cruise Low-Boom Configuration. NASA, TM-2012-217598.

[8] Durston D A, Cliff S E, Wayman T R, Merret, J M, Elmiligui A A, Bangert L S. Near-field sonic boom test on two low-boom configurations using multiple measurement techniques at NASA Ames. AIAA 2011-3333.

[9] Morgenstern J M. How to accurately measure low sonic boom or model surface pressures in supersonic wind tunnels. AIAA 2012-3215, 2012.

[10] Morgenstern J M. Distortion correction for low sonic boom measurement in wind tunnels. AIAA 2012-3216, 2012.

[11] George A R, Seebass R. Sonic Boom Minimization Including Both Front and Rear Shocks. AIAA J. Vol. 9, No.10, Oct. 1971, pp. 2091-2903.

[12] Cliff S, Elmiligui A, Aftosmis M, Thomas S, Morgenstern J, Durston D. Design and Evaluation of a Pressure Rail for Sonic Boom Measurement in Wind Tunnels. Seventh International Conference on Computational Fluid Dynamics (ICCFD7) Big Island, Hawaii, July 9-13, 2012, ICCFD7-2006.

[13] Leng Yan, Liu Zhongchen, Qian Zhansen. Numerical simulation assistant design of the near-field sonic boom signature measurement system for AVIC ARI's FL-60 wind tunnel[C]. HISST 2018, Moscow, Russia, 26th November, 2018.